Journal of Education and Science (ISSN 1812-125X)

www.edusj.mosuljournals.com

Simulation and Analysis of the ^{3}He Detector for Thermal Neutron Detection

R. B. Alkhayat

Department of Physics, Education College for Pure Science, University of Mosul, Mosul, Iraq

Article information

Article history:
Received: January 26, 2023
Accepted: March 13, 2023
Available online: June 01, 2023

Keywords:
Neutron detector
Helium gas
Nuclear interaction
MCNP code
^{3}He(n,p) reaction

Correspondence:
R. B. Alkhayat
Khayatrabee@uomosul.edu.iq

Abstract

This research took advantage of the new features of the MCNPX 6.2 algorithm to model the ^{3}He (n,p) nuclear reaction. The neutron source for the simulation is Am-Be, which emits neutrons with an average energy of 5 MeV. The ^{3}He gas was encapsulated by a thick layer of paraffin. The results obtained have shown that predicting the count values is preferable. additionally, the new versions of MCNPX 6.2 allow the generation of reaction products from proton and triton in addition to the estimated pulse height spectrum of a ^{3}He detector with a considerable detector wall effect. Moreover, it allows studying the dynamics of these reactions as a function of the structure of the ^{3}He detector. The wall effects are small in our modeling design, so the size of the simulation detector is sufficient. The design of the ^{3}He detector is intended to facilitate research into the actions of these reactions.

DOI:10.33899/edusj.2023.138006.1322, ©Authors, 2023, College of Education for Pure Sciences, University of Mosul.

1. Introduction

Neutron detection and spectroscopy frequency employ gas-filled detectors [1]. Gas detectors can detect both fast and slow neutrons through recoil and nuclear reactions, respectively. These detectors mainly use BF3 or ^{3}He, but tubes containing ^{3}He are typically used for thermal neutron detection because proportional counters containing ^{3}He are more sensitive to thermal neutrons than those containing BF3 [2]. Figure 1 shows the various responses of the helium gas detector as a result of the various cross sections of neutrons interacting with ^{3}He at various energies [3]. Due to the high neutron thermal cross-section of ^{3}He and the high reaction energy associated with the neutron capture reaction, proportional counters containing ^{3}He possess the inherent ability to separate neutron events. Triton (191 keV) and proton (573 keV) share the reaction energy, and two particles are assigned to the detection signal [4]–[6]. Consequently, accurate radiation transport calculations can be used to model environmental adjustments [7]–[9]. The measurements can offer crucial observations into the instrument's response, which is essential for the development of new and enhanced nuclear tools. Pulsed radiation sources are intrinsically three-dimensional and time dependent [10]. High precision requires a sufficient description of the source, a comprehensive geometric framework, the most accurate nuclear and atomic data available, and the capability of the tally systems that appropriately describe the detector responses [11], [12]. This study seeks to employ the advanced functionality of the MCNPX 6.2 code to model and analyze a helium-filled counter and the ^{3}He(n,p) reaction to determine response functions for thermal neutron detection in nuclear applications.

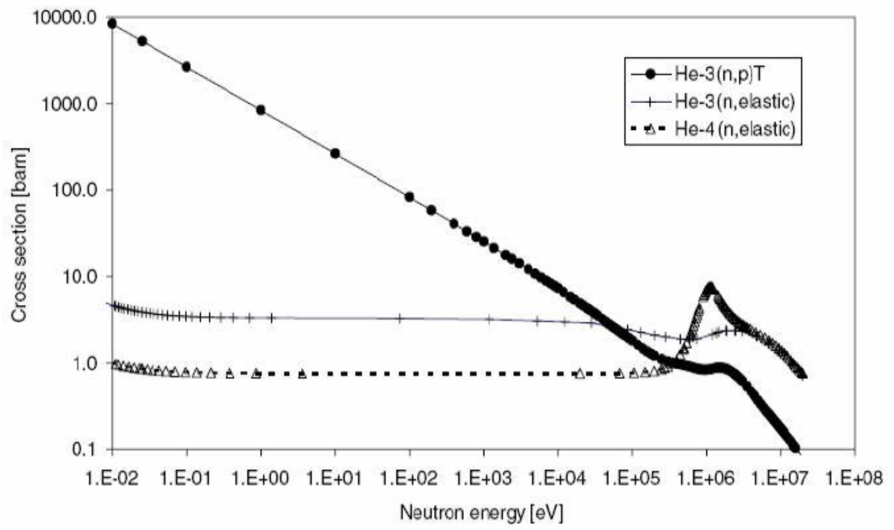

Figure 1. Neutron capture cross-section [3]

2. Computation procedure

MCNP is a Monte Carlo program that can determine the amount of energy sent by ions and light particles in a single particle configuration or when they are connected to other particles in a three-dimensional configuration. The MCNP software and correlated data resources are capable of resolving these complex radiation transport problems. The MCNP simulates the restraint of neutron porosity instruments as one of its applications. Prior to the development of the MCNPx code, it was not possible to examine detector design by generating triton and proton from capture reactions. Now, it is possible to generate all particle types. Neutrons are typically detected by a proportional counter containing ^{3}He. Neutrons are detected in a ^{3}He counter via the nuclear reaction, which produces a proton and a triton that share 765 keV of reaction energy. The particles produced by the nuclear reaction release their energy into the detector material in an opposite direction, causing ionization along particle tracks. MCNP converts neutron fluxes to reaction rates (n, p) utilizing energy functions [1]. It permits comparable count values to be obtained with experimental results. FT8 PHL and F8 totals have been implemented in the calculation of MCNPX. The FT function permits the F8 count to be calculated from energy transfer within a single component using a single F6 tally. Therefore, the energy transfers function (F8) relies on the scores of a different count that also performs since this F8 count is compiled when particle history is complete and the F6 count is collected along the energy path [4]. The energy produced is utilized to divide the total signal peak (F8). Consequently, anticoincidence is regarded [13]–[16]. The neutron source for the simulation is Am-Be, which emits fast neutrons with an average energy of 5 MeV. The ^{3}He gas was confined in a thick layer of paraffin to conduct thermal neutrons. The spectrum of neutron energies for the operated source is illustrated in Figure 2. The detectors are aligned vertically with an anode wire to extend the active area. The geometry of a simulated detector is shown in Figure 3.

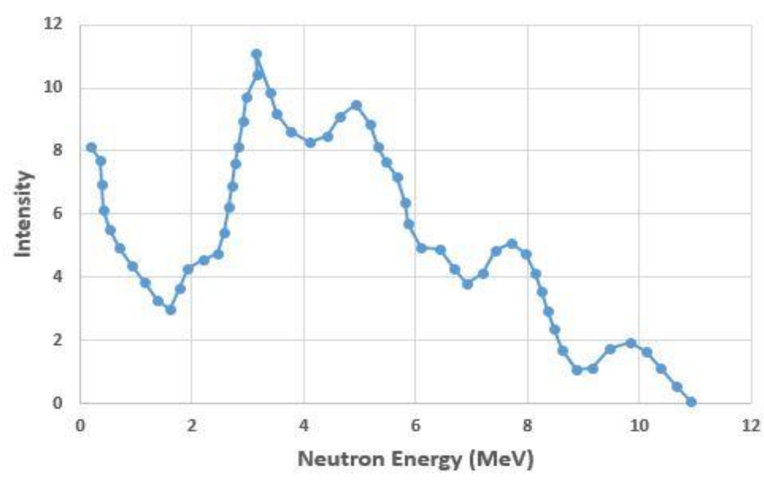

Figure 2. Am-Be neutron source energy spectrum [17]

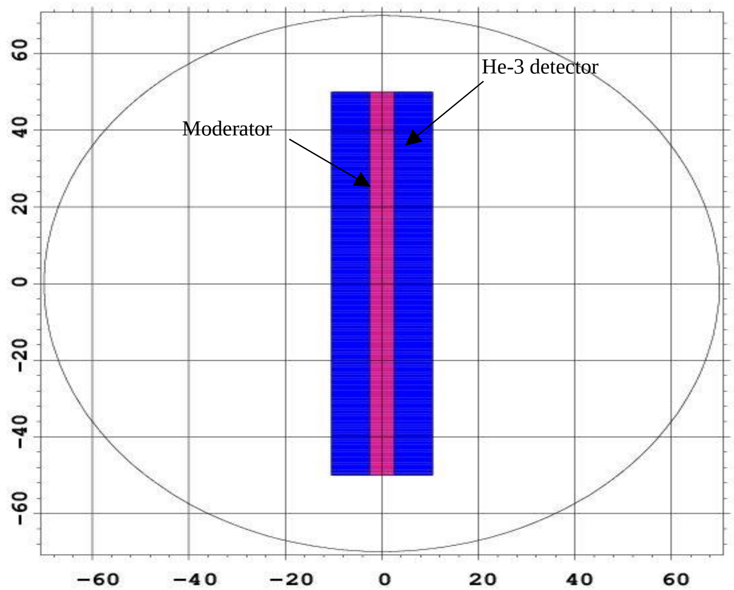

Figure 3. Schematic diagram of the MCNPX 6.2-modeled ^{3}He detector in xy plane.

3. Results and Discussion

As previously stated, the energy released corresponds to the sum of the proton and triton energies. The (n, p) reaction and elastic scattering constitute the ^{3}He proportional counter-detection mechanism followed by the reaction
$n + {}^3\text{He} \longrightarrow {}^3\text{H} + {}^1\text{H} + 0.764$ MeV.

Figure 4 illustrates the distribution of protons and tritons energy. As can be observed, the energies deposited by the proton and triton are 573 keV and 191 keV, respectively. The ^{3}He pulse height spectrum is illustrated in Figure 5. All the energy of the reaction products (protons and tritons) is transferred to the detector gas only when the detector tube is large enough. In this case, the reactions are sufficiently distant from the detector wall. As the tube is no longer disproportionately large concerning the proton and triton range produced by the reaction, the entire reaction energy no longer accumulates in the gas. In this instance, the reaction products collide with the detector walls, resulting in a diminished pulse. This effect is termed the wall effect in gas detectors. This effect is responsible for the two discontinuities as shown in Figure 5.

The reaction products must encounter opposite directions because the approaching neutron has negligible momentum. If a proton collides with the detector wall, the triton will be deflected far from the detector wall and will probably deposit all of its energy into the detector material. The proton then transfers some of its energy to the detector. This reaction could occur somewhere between zero and the entire proton scope on the detector wall. Energy injected into a detector can range between E_{3H} and $E_{3H} + E_p$. Since the probability of the reaction occurring in any of the possible locations is approximately equal, the energy will be divided approximately evenly between these two products.

In contrast, the proton energy is typically absorbed within the detector when the triton collides with the detector wall. Consequently, we anticipate losing a single product with every interaction because of the interaction with detector walls. The triton deposits a portion of its energy when it hits a detector wall, whereas the proton is completely absorbed. Using the same kind of reasoning, you can show that the energy put into the gas is between E_p and E_{3H}. The total amount of energy deposited when one of the reaction products hits a detector wall is the same as if you just added the two cases together.

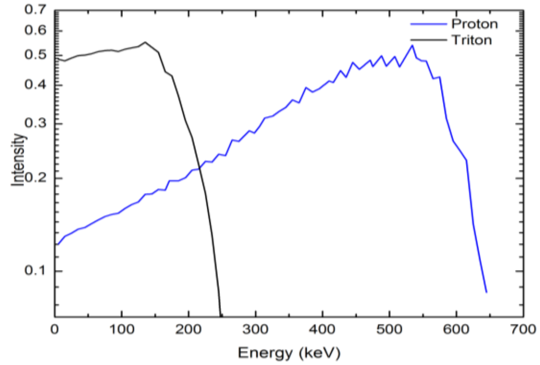

Figure 4. The distribution of proton and triton energy

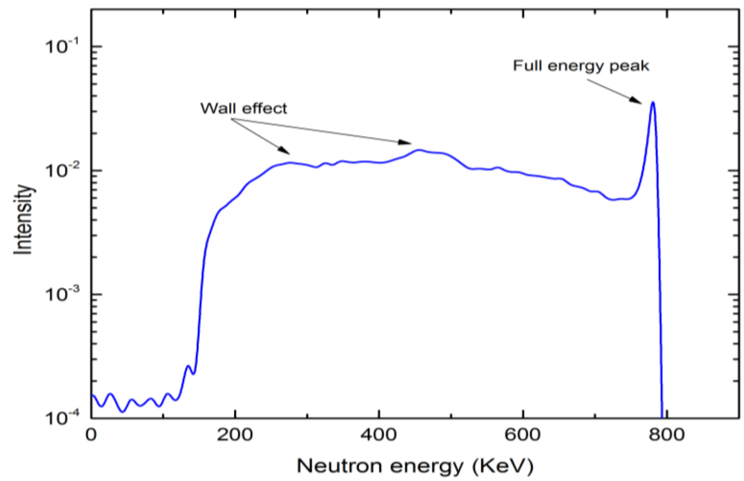

Figure 5. Pulse height spectrum of the ^{3}He detector

4. Conclusion

This work employed the latest functionality of the MCNPX 6.2 simulation code to predict the ^{3}He (n,p) nuclear reaction, which is advantageous for nuclear achievements. The results obtained have shown that predicting count values is straightforward. Furthermore, the new MCNPX 6.2 capabilities enable the generation of reaction products (triton and proton) as well as the estimation of the pulse height spectrum using a ^{3}He detector with a notable wall effect. The purpose of the design of the ^{3}He detector is to permit studies into the behavior of these reactions. The wall effects are minimal, so the size of the detector adopted for simulation is adequate.

5. Acknowledgments

Our distinguished thanks go to the University of Mosul, the College of Education for Pure Science, and the Department of Physics for supporting this work.

6. References

[1] E. Dietz, M. Matzke, W. Sosaat, G. Urbach, and M. Weyrauch, “Neutron response of an 3He proportional counter,” *Nucl. Instruments Methods Phys. Res. Sect. A Accel. Spectrometers, Detect. Assoc. Equip.*, vol. 332, no. 3, pp. 521–528, Aug. 1993.

[2] D. H. Lee, B. H. Park, Y. K. Kim, and G. D. Kim, “A Study on performance of 3 He and 4 He proportional counter for thermal neutron detection,” pp. 635–636, 2008.

[3] “ENDF/B-VI evaluated nuclear data file. Data base version 2022. www.nndc.bnl.gov/exfor/endfoo.htm.” .

[4] M. Weyrauch, A. Casnati, P. Schillebeeckx, and M. Clapham, "Use of 4He-filled proportional counters as neutron spectrometers," *Nucl. Instruments Methods Phys. Res. Sect. A Accel. Spectrometers, Detect. Assoc. Equip.*, vol. 403, no. 2–3, pp. 442–454, Feb. 1998.

[5] A. Pietropaolo *et al.*, "Neutron detection techniques from μeV to GeV," *Phys. Rep.*, vol. 875, pp. 1–65, Sep. 2020.

[6] C. Eleon, B. Perot, C. Carasco, D. Sudac, J. Obhodas, and V. Valkovic, "Experimental and MCNP simulated gamma-ray spectra for the UNCOSS neutron-based explosive detector," *Nucl. Instruments Methods Phys. Res. Sect. A Accel. Spectrometers, Detect. Assoc. Equip.*, vol. 629, no. 1, pp. 220–229, 2011.

[7] A. Azbouche, M. Belgaid, and H. Mazrou, "Monte Carlo calculations of the HPGe detector efficiency for radioactivity measurement of large volume environmental samples," *J. Environ. Radioact.*, vol. 146, pp. 119–124, Aug. 2015.

[8] R. P. Nathan, P. J. Thomas, M. Jain, A. S. Murray, and E. J. Rhodes, "Environmental dose rate heterogeneity of beta radiation and its implications for luminescence dating: Monte Carlo modelling and experimental validation," *Radiat. Meas.*, vol. 37, no. 4–5, pp. 305–313, Aug. 2003.

[9] H. Jäderström, W. F. Mueller, V. Atrashkevich, and A. S. Adekola, "True coincidence summing correction and mathematical efficiency modeling of a well detector," *Nucl. Instruments Methods Phys. Res. Sect. A Accel. Spectrometers, Detect. Assoc. Equip.*, vol. 784, pp. 264–268, Jun. 2015.

[10] Q. Zhang *et al.*, "GMAC: A Geant4-based Monte Carlo Automated computational platform for developing nuclear tool digital twins," *Appl. Radiat. Isot.*, vol. 192, p. 110579, Feb. 2023.

[11] T. Goričanec, D. Kotnik, Ž. Štancar, L. Snoj, and M. Kromar, "Predicting Ex-core Detector Response in a PWR with Monte Carlo Neutron Transport Methods," *EPJ Web Conf.*, vol. 225, p. 03007, 2020.

[12] M. Jeong and M. D. Hammig, "Comparison of gamma ray localization using system matrixes obtained by either MCNP simulations or ray-driven calculations for a coded-aperture imaging system," *Nucl. Instruments Methods Phys. Res. Sect. A Accel. Spectrometers, Detect. Assoc. Equip.*, vol. 954, p. 161353, Feb. 2020.

[13] A. Haghighat, *Monte Carlo methods for particle transport*. Crc Press., 2020.

[14] S. K. Aghara, S. I. Sriprisan, R. C. Singleterry, and T. Sato, "Shielding evaluation for solar particle events using MCNPX, PHITS and OLTARIS codes," *Life Sci. Sp. Res.*, vol. 4, pp. 79–91, Jan. 2015.

[15] P. Sauvan, J. Sanz, and F. Ogando, "New capabilities for Monte Carlo simulation of deuteron transport and secondary products generation," *Nucl. Instruments Methods Phys. Res. Sect. A Accel. Spectrometers, Detect. Assoc. Equip.*, vol. 614, no. 3, pp. 323–330, Mar. 2010.

[16] A. Mohammed-Ali, R. B. Alkhayat, M. M. Yousif, M. Al-Jubbori, H. H. Kassim, and F. I. Sharrad, "Description of Nuclear Properties for 114-128Cd Isotopes," *Rev. Mex. Física*, vol. 68, no. 6 Nov-Dec, pp. 1–8, 2022.

[17] A. D. Vijaya and A. Kumar, "The neutron spectrum of AmBe neutron sources," *Nucl. Instruments Methods*, vol. 111, no. 3, pp. 435–440, 1973.

ربيع بهنام الخياط

قسم الفيزياء، كلية التربية للعلوم الصرفة، جامعة الموصل، الموصل، العراق

الخلاصة

الهدف من البحث هو الاستفادة من الميزات الجديدة لخوارزمية MCNPX 6.2 لمحاكاة التفاعل النووي $^{3}He(n,p)$. المصدر النيوتروني المستخدم لمحاكاة التفاعل النووي هو Am-Be الذي يبعث نيوترونات بمتوسط طاقة 5 MeV .تم تغليف عداد ^{3}He الغازي بطبقة سميكة من البارافين لابطاء النيوترونات السريعة. تشير النتائج الى أنه من الأفضل التنبؤ بقيم العد للنبضات. بالإضافة إلى ذلك ، تسمح الإصدارات الجديدة من MCNPX 6.2 بايجاد طاقة كل من التريتيوم و البروتون بالإضافة إلى طيف ارتفاع النبضة للكاشف ^{3}He مع تأثير جدار انبوبة الكاشف. علاوة على ذلك ، فإنه يسمح بدراسة ديناميكيات هذه التفاعلات كدالة لهيكلية الكاشف ^{3}He .ابعاد الكاشف المستخدم في المحاكاة كافٍ لامتصاص التفاعلات النووية من البروتونات والتريتيونات المتولدة لان تأثيرات اصطدام هذه النوى المتولدة مع جدار الكاشف صغيرة. لانه مثل هذه التفاعلات مهمة في الفيزياء النووية وتستخدم في كثير من المجلات العلمية مثل منتجات النفط والغاز والسبب في ذلك لانه يمكن لكواشف الغاز اكتشاف النيوترونات السريعة والبطيئة من خلال الارتداد والتفاعلات النووية.